ACS Catalysis

Research Article

pubs.acs.org/acscatalysis

Toward Functional Polyester Building Blocks from Renewable Glycolaldehyde with Sn Cascade Catalysis

Michiel Dusselier,*[,†] Pieter Van Wouwe,[†] Sanne De Smet,[‡] Rik De Clercq,[†] Leander Verbelen,[§] Peter Van Puyvelde,[§] Filip E. Du Prez,[‡] and Bert F. Sels*[,†]

[†]Center for Surface Chemistry and Catalysis, Katholieke Universiteit Leuven, Kasteelpark Arenberg 23, 3001 Leuven, Belgium

[‡]Department of Organic Chemistry, Polymer Chemistry Research Group, Ghent University, Krijgslaan 281, S4-bis, 9000 Ghent, Belgium

[§]Department of Chemical Engineering, Katholieke Universiteit Leuven, Willem de Croylaan 46, 3001 Leuven, Belgium

Supporting Information

ABSTRACT: Having been inspired by formose-based hypotheses surrounding the origin of life, we report on a novel catalytic route toward a series of recently discovered four-carbon α-hydroxy acids (AHA) and their esters from accessible and renewable glycolaldehyde (GA) in various solvents. The synthesis route follows a cascade type reaction network, and its mechanism with identification of the rate-determining step was investigated with in situ ^{13}C NMR. The mechanistic understanding led to optimized reaction conditions with higher overall rates of AHA formation by balancing Brønsted and Lewis acid activity, both originating from the tin halide catalyst. An optimal H^+/Sn ratio of 3 was identified, and this number was surprisingly irrespective of the Sn oxidation state. Further rate enhancement was accomplished by adding small amounts of water to the reaction mixture, boosting the rate by a factor of 4.5 compared with pure methanol solvent. The cascade reaction selectively yields near 60% methyl-4-methoxy-2-hydroxybutanoate (MMHB). In the optimized rate regime in methanol, an initial TOF of 7.4 $mol_{GA}\ mol_{Sn}^{-1}\ h^{-1}$ was found. In sterically hindered alcohols (isopropyl alcohol), the rate of AHA formation was even higher, and the corresponding vinyl glycolate esters arose as the main product. Vinyl glycolic acid, 2,4-dihydroxybutanoic acid, and its lactone were formed significantly in nonprotic solvent. The corresponding AHAs have serious potential as building blocks in novel biobased polymers with tunable functionality. The incorporation of vinyl glycolic acid in polylactic acid-based polyesters is illustrated, and postmodification at the vinyl side groups indeed allows access to a range of properties, such as tunable hydrophilicity, which is otherwise difficult to attain for pure poly(L-lactic acid).

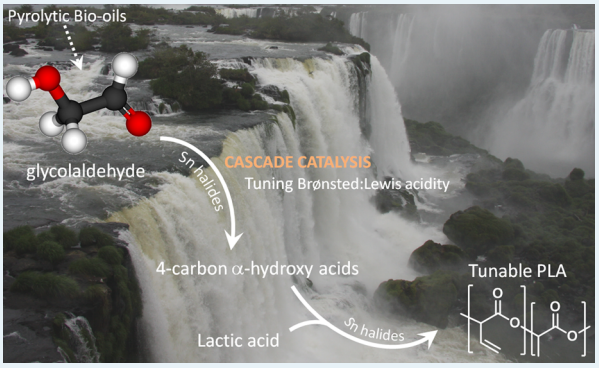

KEYWORDS: *homogeneous catalysis, biomass, building blocks, glycolaldehyde, α-hydroxy acids, biodegradable polymers, polylactic acid*

INTRODUCTION

α-Hydroxy acids (AHAs) and their esters are of great appeal as platform chemicals[1−3] in the portfolio of renewable derived solvents and as building blocks for polyesters.[1,4,5] Lactic acid,[1] for instance (a three-carbon AHA), is a rapidly growing commodity chemical; its ethyl ester (ethyl lactate[6,7]) is becoming a renowned green solvent, and polylactic acid (PLA) is currently one of the top volume bioplastics.[8,9] Being renewable[10] and biodegradable,[11−13] such polyesters not only are useful to replace petroleum-derived plastics in certain applications, but also have a promising future in biomedical and in vivo applications because of their biocompatibility.[14,15] Their ever increasing popularity is due in part to rising concern over the use of depleting fossil feedstock for the production of classic polymers. Moreover, most of these polymers are nondegradable and lie at the origin of a huge waste problem, sadly exemplified by plastic scrap covering our remotest islands and oceans.[14,16−18] Traditional poly(L-lactic acid) (PLLA) has many good features, but also some limitations:[8] it is a brittle polymer with poor elongation at break and lacks reactive side chain groups for chemical modification. Moreover, PLLA is often considered too hydrophobic, causing inflammatory responses when applied in vivo.[12,19]

Recently, intriguing four-carbon AHAs were discovered in small amounts during the chemocatalytic conversion of hexoses and hemicellulosic sugars to alkyl lactates with Sn-based zeolites[20,21] and with our Sn-containing silica/carbon composite catalysts.[5] The origin of these esters, namely, MVG (methyl vinyl glycolate) and MMHB (methyl-4-methoxy-2-hydroxybutanoate), was attributed to the presence of tetrose sugars,

Received: April 19, 2013
Revised: June 23, 2013
Published: June 25, 2013

formed by the retro-aldol splitting of glucose (Scheme 1). Because of their structure, these AHAs could offer a solution to

Scheme 1. Overview of the Synthesis of Four-Carbon AHAs from Tetroses[22] and Glycolaldehyde (this work) and Some of the Demonstrated Tunable (PLA-based) Copolymers

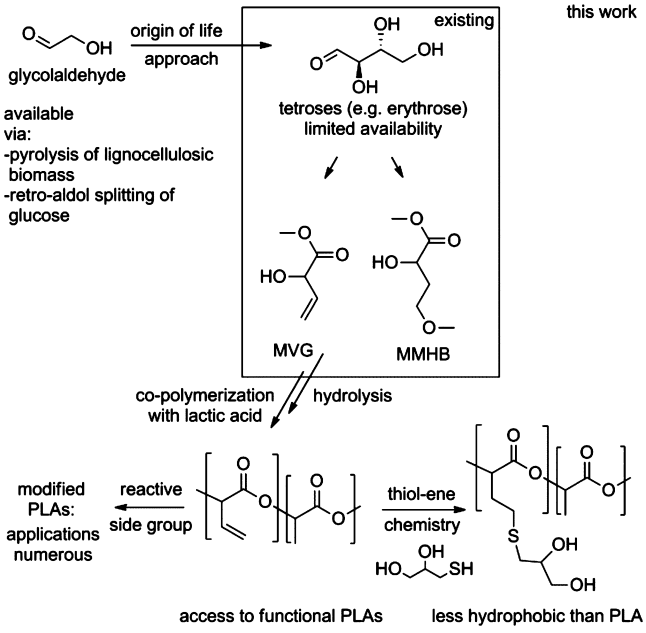

overcome certain of the PLA limitations by coincorporation: MVG has a vinyl (and thus, easy access to functionalization) instead of the methyl group in lactic acid, whereas MMHB possesses a 4-methoxy substituent, a more polar tail group. Moreover, the search for new catalytic routes toward such molecules is interesting because they are very rare in nature, in contrast to lactic acid. Recently, we delivered mechanistic insight into the conversion of tetrose sugars to these novel AHAs platform molecules with Sn halide catalysts.[22] Especially, MMHB was shown to be synthesized in high yield in methanol under mild conditions from erythrulose and erythrose in one step, involving many different types of reactions, as catalyzed by Sn halides. Reported yields to MVG in this report were rather low.

Although very useful for providing mechanistic evidence and elucidating reaction pathways, the tetroses in previous study are very expensive and not accessible on a large scale.[22] Glycolaldehyde (GA),[23] the "two-carbon" sugar, however, is encountered in high yields when converting glucose via retro-aldol splitting under subcritical hydrothermal conditions,[24] and more significantly, it is one of the major constituents of bio-oils obtained via pyrolysis of biomass residue.[25,26] Up to 10 wt % yield of GA can be found in such oils obtained from the pyrolysis of cellulose, nature's most abundant renewable biomass resource.[27−34] These yields are relevant considering the nonselective nature of the pyrolysis process and the overwhelming availability of the feedstock. Moreover, successful efforts have been made recently toward GA isolation from such complex bio-oils.[35]

In a totally different context, in search for the origin of life, the formose-based synthesis of sugars starting from formaldehyde or GA (even found in outer space[36,37]) with the help of mineral-derived alkali, borates, or amino acids is offering a likely explanation for the rise of complex organic molecules and ribose-sugar-based life under credible prebiotic conditions.[37−40] The formose process entails several aldol reactions, eventually leading to complex sugar mixtures and tars.[41−43] Borates[39,44] and silicates[45] were found to stabilize (especially) pentoses from these reaction mixtures, thereby possibly directing the unselective formose reaction. In this way, for example, borate-bound sugars are excluded to undergo further aldol condensation.

Inspired by this approach, and in the light of the future availability of GA via biomass pyrolysis, we demonstrate here the one-pot catalytic conversion of GA to four-carbon AHA (esters) according to a complex cascade network. The unselective aldol-based sugar synthesis is hereto combined with the Sn-based homogeneous catalytic transformation of tetroses to AHAs. In this way, the formation of unwanted larger carbohydrates from tetroses and GA is circumvented. With the help of in situ NMR, key insights into the reaction mechanism and its catalytic needs are unravelled. Finally, the potential of such derived AHA monomer building blocks is proved for the first time by their copolymerization with lactic acid, leading to a new range of tunable PLA based polymers with interesting properties and easy access to functionalization, for instance, by thiol/-ene chemistry (on polylactic acid-co-vinyl glycolate), as visualized in Scheme 1.

METHODS

Catalytic Tests. Experiments were performed in 10 mL-thick-walled glass vial reactors. In a typical experiment, 0.0025 mol of glycolaldehyde (0.150 g, dimeric form, Sigma-Aldrich) was combined with 1.25×10^{-4} mol of Sn catalyst; for instance, 43.8 mg in the case of $SnCl_4 \cdot 5H_2O$ (Acros), in 2 mL of solvent (methanol, ethanol, IPA, methanol/water). Naphthalene (50 mg) was used as the internal (or external) standard. A magnetic stirring bar was then added, and the glass vials were closed by crimp cap with a septum and placed into a multivial heating block at 363 K. The mixture was allowed to react for certain amounts of time ranging from 5 min to 26 h, depending on the progress under continuous magnetic stirring. To quench intrinsic HCl-derived Brønsted acidity (BA), precise amounts of Dowex Monosphere 550A anion exchange resin based on a quaternary amine in its OH^- form were added to the catalytic mixture. To add extrinsic HCl, a solution in methanol was prepared and added. To determine the quenching capacity of such a resin, it was fully exchanged under excess NaOH, thoroughly washed, and titrated (anion exchange capacity of 1.5 mmol/g).

Analysis: Methyl-4-methoxy-2-hydroxybutanoate (MMHB), methyl vinyl glycolate (MVG), and their alkyl analogues and glycolaldehyde dimethyl acetal (GADMA) were analyzed by gas chromatography on a 30 m Agilent HP-5 column and on a chiral 25 m Agilent WCOT fused-silica CP-Chirasil-DEX CB capillary column, both equipped with an FID detector and ChemStation software. A chromatogram is illustrated in the Supporting Information (Figure S6B) Product yields were calculated via internal standards. Sensitivity factors were obtained by calibration with commercial standards (MVG, 96%, TCI Europe; GADMA; 98% Alfa Aesar) or obtained by ECN-based calculations,[46] because of a lack of commercial standard (for MMHB and alkyl analogues of MMHB and MVG). Identification of the reaction products was carried out by GC/MS analysis with electronic ionization, ^{13}C NMR, ^{1}H NMR, and GC based on retention times of commercial reference chemicals. A Hewlett-Packard 5989A mass spec-

dx.doi.org/10.1021/cs400298n | ACS Catal. 2013, 3, 1786−1800

trometer using electronic ionization was used to further identify the glycolaldehyde hemiacetal.

In Situ Studies. Typically, 0.05 g of glycolaldehyde (dimeric form, Sigma-Aldrich) was dissolved in either 0.6 mL of CH_3OH, CD_3OD, isopropyl alcohol, acetonitrile, or dimethyl sulfoxide (DMSO) or mixtures thereof with H_2O or D_2O, and a ^{13}C NMR spectrum was recorded. Then this mixture was added to a $SnCl_4{\cdot}5H_2O$-containing vial. Different GA/Sn ratios were used (2:1, 5:1, 10:1). As soon as the mixture was homogeneous, it was transferred back to the 5 mm Norell tube and lowered into a Bruker Avance II-plus 600 MHz spectrometer equipped with a BBO probe or a Bruker Avance 400 MHz spectrometer with a BBI probe. The sweep was put off in the case of nondeuterated solvents. In this way, the first accumulation of 128 scans (6−7 min) (or 256 scans, depending on the signal-to-noise ratio and the concentration) could be recorded ∼2.5 min after mixing. The number of desired acquisitions was put in sequence and mostly run overnight. For temperatures other than 298 K (usually 333 K), the spectrometer was allowed to reach the temperature and equilibrate before the sample was loaded. A Bruker Avance 300 MHz equipped with a BBO probe was used for standard NMR measurements. Topspin 2.1 Software was used for controlling the spectrometers and analyzing the results.

Polymerization via Polycondensation. MVG (97%, TCI Europe) was filtered over activated basic aluminum oxide (Sigma-Aldrich) to retain possible carboxylic acid impurities. For the synthesis of polylactic acid-co-vinyl glycolate (7%), 0.7 g of MVG was dissolved in 20 mL of Millipore water, and 0.7 g of Amberlyst 15, a strong acidic cation exchange resin, was added as a hydrolysis catalyst (1 g). This mixture was continuously stirred in an oil bath kept at 353 K. The mixture was left to react until complete conversion of MVG, as analyzed by GC. The resulting vinyl glycolate monomer (2-hydroxy-3-butenoic acid) was ascertained by ^1H and ^{13}C NMR. Amberlyst wet 15 (Sigma-Aldrich) was filtered off, and the excess of water was slowly evaporated with a gentle nitrogen flow while keeping the mixture at 333 K. The dried monomer (4.7 mmol, 0.48 g, oil) was mixed with 42.3 mmol of lactic acid (4.15 g of a 90 wt % aqueous solution, Sigma-Aldrich) to obtain a monomer composition of vinyl glycolate/lactic acid of 1:10. To this, *p*-xylene was added to obtain a 50 wt % monomer mixture as well as 0.2 wt % (on monomer) of the $SnCl_2{\cdot}2H_2O$ polycondensation catalyst, according to Kim et al.[47] The reaction vessel was equipped with a Dean−Stark trap (filled before reaction with *p*-xylene) and left to reflux in an oil bath at 160 °C for 72 h. The resulting mixture was dissolved in $CHCl_3$ and precipitated in excess cold CH_3OH (nonsolvent). The resulting polyester was filtered off and dried under vacuum. Reference poly(L-lactic acid) was made in exactly the same manner.

Polymer Characterization. ^1H-, ^1H-COSY-, and ^1H-/^{13}C-HSQC were recorded in $CDCl_3$ on Bruker Avance 400 and 300 MHz spectrometers. In addition, ^{13}C NMR and ^{13}C-APT-NMR were measured on a Bruker AM500 MHz spectrometer. Thermal gravimetric analysis (TGA) was performed on the polymer powders while heating them at a rate of 10 K/min under N_2 atmosphere using a TGA Q500 (TA Instruments) equipped with an automatic sampler. Differential scanning calorimetry (DSC) experiments were performed with a DSC Q2000 (TA Instruments) by cycling between 283 and 483 K at heating/cooling rates of 10 K/min under N_2 atmosphere. Size exclusion chromatography (SEC) was performed using a Varian PLGPC50plus instrument, using a refractive index detector, equipped with two Plgel 5 μm MIXED-D columns kept at 40 °C. Polystyrene standards were used for calibration, and THF, as eluent at a flow rate of 1 mL/min. Samples were injected using a PL AS RT autosampler. Static contact angle measurements were performed with double deionized water on polymer coated glass slides with a KSV NIMA CAM200 setup and its software. Hereto, the polymers were spin-coated from a 5 wt % solution in $CHCl_3$ or THF on a thin glass preparation slide for 1 min at a rate of 1000 rpm attained in 2 s. The slides were dried overnight at room temperature. Per slide, 3 drops were measured, and during measurement, 2 subdrops were added. Thirty seconds after adding each subdrop, the photographed droplet was fit according to the Young−Laplace equation, and the static contact angle was calculated. At least 2 slides per polymer were prepared. Standard deviations were calculated.

Thiol-ene Functionalization of Polymers. A typical thiol-ene reaction was performed as follows: Functionalized polymer PLLA-co-VG (12% vinyl) (100 mg; 0,19 mmol alkene) was dissolved in dry THF (1.0 mL). Benzyl mercaptan (99% Sigma-Aldrich, 0.38 mmol) and 2,2-dimethoxy-2-phenyl-acetophenone (99% Sigma-Aldrich, 5.0 mg/mL) as photo-initiator were added, and the solution was degassed for 30 min with N_2. In another case, 1-thioglycerol (>97%, Sigma-Aldrich) was used. The reaction mixture was irradiated with UV-light (365 nm) for 5 h at ambient conditions. The functionalized polymer was collected by precipitation in cold methanol or diethyl ether and dried prior to analysis.

RESULTS

Occurrence of Glycolaldehyde in Reaction Conditions. Commercial glycolaldehyde (GA) is found in its crystalline dimeric form (**1** in Scheme 2). This dimer is said to decompose thermally into monomeric GA (**2** in Scheme 2). The free aldehyde group, however, is rarely encountered because its main occurrence greatly depends on the solvent. In water, for instance, its hydrate (**2″**) is the most encountered form at standard conditions, and this form is easily detected in

Scheme 2. Occurrence of GA (2) and Its Basic Aldol Reaction in Water (A) and Its Occurrence in Methanol (B)

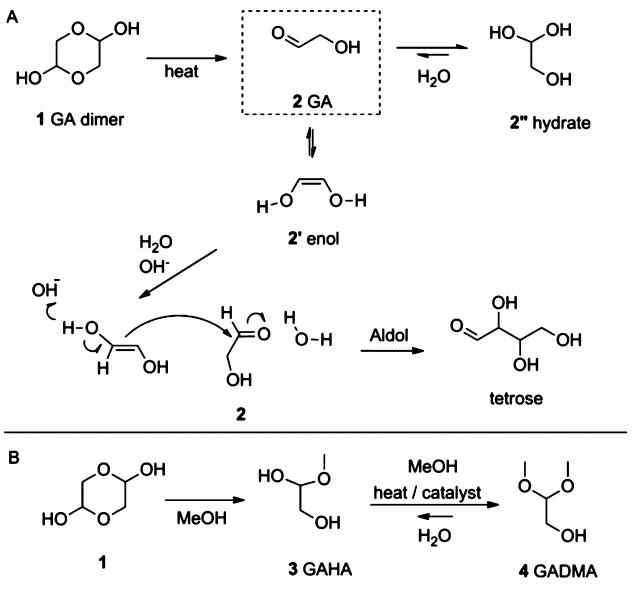

dx.doi.org/10.1021/cs400298n | ACS Catal. 2013, 3, 1786−1800

^{13}C NMR.[48,49] In light of the origin of life, in length reviewed by Benner et al. in a recent perspective,[37] it was shown that GA, when incubated in a borate buffer (pH 10.4) at 338 K for 1 h, led to the formation of mainly threose and erythrose, two tetrose sugars, in a yield of 86%.[39] The aldol reaction arose from the basicity of the medium (free OH^-), and the mechanism of this aldol reaction is generally known as the enolate mechanism, involving the base-catalyzed enolization of GA, transforming it into a nucleophile (seen as **2′** in Scheme 2), which attacks the aldehyde carbon of another GA molecule, with the formation of a tetrose as the result (an aldose: threose or erythrose). This reaction proves the ease of condensing GA toward higher sugars in basic media, as illustrated in Scheme 2A, and it is the main mechanism behind the formose reaction.[42]

In the same context, Kofoed et al. have studied GA conversion in the absence of a base, catalyzed by a $Zn^{II}(proline)_2$ Lewis acidic catalyst (proposed to be a likely metalloenzyme precursor) under credible prebiotic conditions.[50] The aldol reactivity was postulated to be catalyzed by the Lewis acidic Zn^{II} center chelated with a glycolaldehyde enolate. Burroughs et al. showed that esters of proteinogenic amino acids (e.g., *N*-methyl leucine ethyl ester) were also able to perform this reaction via the enamine aldol mechanism in similar circumstances.[51]

The ultimate challenge for using GA as biomass feedstock for the formation of four-carbon α-hydroxy acid esters (AHA) is the cascade coupling of the aldol reaction of GA to tetroses with the subsequent selective conversion to MMHB and MVG. The established conversion of tetroses to AHA-containing compounds with Sn halides salts is preferably carried out in alcoholic media to avoid side product formation, side-reactions with the formed carboxylic acid group and the formation of tin(hydr)oxides.[22]

The occurrence of GA in methanol (Scheme 2B) plays a crucial role in the conversion of GA to AHAs and was therefore studied first with (in situ) ^{13}C NMR. The spectral evidence is presented in Figure 1. Part i of Figure 1 thus shows the spectrum of the crystalline dimeric form **1**, immediately after dissolution in CH_3OH at 298 K. When heating such a mixture for only 5 min at 363 K, the cyclic dimer **1** undergoes a rapid transformation to glycolaldehyde hemiacetal (GAHA, **3** in Scheme 2), and its three signals—98, 65, and 54 ppm—are the only ones found, as seen in Figure 1, part ii. During very long incubation at 363 K, the diagnostic chemical shifts at 98 and 65 ppm gradually diminished in favor of two new signals at 105 and 62 ppm, whereas the signal at 54 ppm increased. This change in ^{13}C NMR signals corresponds to the formation of the dimethyl acetal of GA (GADMA, **4** in Scheme 2), which has overlapping methyl signals at 54 ppm, as seen in Figure 1, part iii, and its chemical shifts were perfectly in agreement with a commercial standard. This transformation (GAHA **3** into GADMA **4**) is, however, very slow in pure methanol at 363 K, and it does not even seem to occur within 5 days of incubation at 298 K. Thus, as seen in Scheme 2B, formation of GADMA from GAHA requires sufficient time and heat or an appropriate catalyst to accelerate the second acetalization. Such acetalization reactions are reversible and typically catalyzed by Brønsted (or Lewis) acids.[52] This is evidenced by the rapid formation of GADMA, within 30 min, when GA dimer was dissolved at 298 K in methanol containing HCl (in situ ^{13}C NMR spectral sequence for 10:1 GA/H^+; see Supporting Information Figure S1). The effect of Sn halide catalysts on the occurrence of GA was therefore also studied with an identical GA solution in the presence of $SnCl_4{\cdot}5H_2O$ in a 10:1 GA/Sn molar ratio in the spectrometer at 298 K. The rapid transformation of GAHA to GADMA could again clearly be witnessed by in situ NMR and took about 90 min to completion; in fact, the last spectrum of this sequence is shown in Figure 1, part iii. The same experiment carried out at 333 K displayed nothing but GADMA **4** after 2 min, proving the catalytic effect of $SnCl_4{\cdot}5H_2O$ halides.

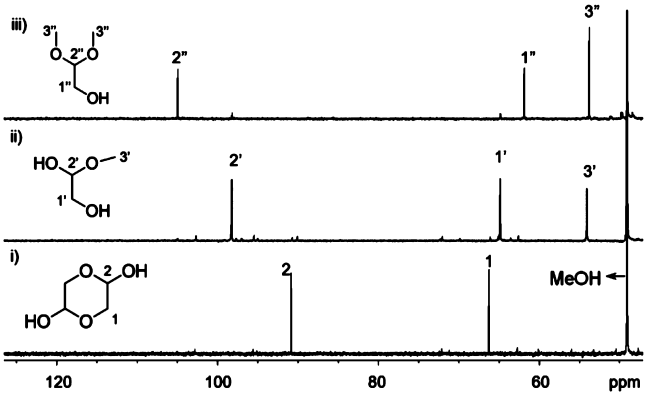

Figure 1. (i) GA dimer **1**, 2 min after dissolution in CH_3OH at 298 K. (ii) Such mixture heated at 363 K for 5 min: formation of GAHA **3**. (iii) GA dimer **1** dissolved in CH_3OH containing 10 mol % of $SnCl_4{\cdot}5H_2O$ after 90 min at 298 K: GADMA **4**.

In conclusion, GA dimer **1** readily converts to the hemiacetal GAHA **3**, but it takes over 24 h to convert **3** further into diacetal GADMA **4** without catalyst at 363 K in methanol. The second acetalization is very fast in the presence of HCl or $SnCl_4{\cdot}5H_2O$ catalysts, even at room temperature. In the latter case, the acetalization activity likely originates from Brønsted acidity by dissociation of chloride ligands with formation of HCl. At 333 K, with such a catalyst, acetal **4** is formed immediately from **1** in CH_3OH.

Catalytic Cascade: Proof of Concept. To investigate the ability of Sn halides and other soluble model catalysts to assist the overall reaction of two GA molecules into four-carbon AHAs (seen in Scheme 1) in alcoholic media, concentrated solutions of GA dimer **1** were contacted with catalytic amounts of Sn, Al, and Cr halides. These catalysts were recently proposed in for the conversion of tetroses to AHAs.[22] The experiments were performed with 1.25 M GA in methanol at 363 K for ~20 h. An intermediate sample was taken after 1 h of reaction for a kinetic analysis. This reaction condition closely matches the one used in our earlier study for the conversion of tetrose sugars in CH_3OH (0.625 M tetrose at 363 K).[15] The results of the screening are found in Table 1. Sn halides are, indeed, able to perform the whole cascade reaction in CH_3OH, yielding between 50 and 60% of MMHB **9** (Scheme 3) from **1** after 20 h of reaction. As seen in entries 6 and 8, both Sn^{II} and Sn^{IV} produce **9**, whereas MVG is only a minor product. Starting from a tetrose feedstock (erythrose) instead of **1**, as seen in entry 11, similar yields were obtained, albeit much faster.

The successful catalytic reactions prompted us to monitor the reaction evolution in time in the presence of the tin catalysts. One hour points are shown in entries 5 and 7, and the kinetic plot is presented in Figure 2. The latter displays that 80% of the final yield (viz., 58% after 20 h) is already obtained after 7 h of reaction. The primary product of the reaction

dx.doi.org/10.1021/cs400298n | ACS Catal. 2013, 3, 1786−1800

Table 1. Screening for the Conversion of Glycolaldehyde to GADMA 4 and α-Hydroxy Acid Esters in CH_3OH[a]

entry	catalyst	t (h)	GADMA (%)	MMHB (%)	MVG (%)
1		26	47	0	0
2	HCl	1	72	0	0
3	HCl	22	56	0	0
4	NaOH	20	0	0	0
5	$Sn^{IV}Cl_4{\cdot}5H_2O$	1	54	10	<1
6	$Sn^{IV}Cl_4{\cdot}5H_2O$	20	3	58	3
7	$Sn^{II}Cl_2{\cdot}2H_2O$	1	51	14	<1
8	$Sn^{II}Cl_2{\cdot}2H_2O$	21	1	55	4
9	$Al^{III}Cl_3{\cdot}6H_2O$	20	47	7	0
10	$Cr^{III}Cl_3{\cdot}6H_2O$	20	71	<1	0
11[b]	$Sn^{IV}Cl_4{\cdot}5H_2O$	1		50	2

[a]Reactions at 363 K with 1.25 M GA (provided as dimer, **1**) in MeOH. GC-based yields; 5 mol % of catalyst (20 mol % for HCl, 10 mol % for NaOH). [b]Reaction on 0.625 M of erythrose in CH_3OH, 10 mol % of catalyst.

proved to be the acetal **4**. This is in agreement with the ^{13}C NMR data mentioned above, where its formation from GA dimer **1** was noticed instantaneously upon contact with $SnCl_4{\cdot}5H_2O$ in methanol at 333 K.

Reaction with HCl, a model Brønsted acid catalyst, led to neither MMHB **9** nor MVG formation, and the main product was the acetal GADMA **4** (entries 2 and 3), in addition to other acetalization products, such as 1,1,2-trimethoxyethane and tetramethoxyethane. A reaction with catalytic amounts of base (viz., NaOH) yielded no GC-detectable products. Other Lewis acids (viz. Al^{III} and Cr^{III} halides; entries 9 and 10) appeared unable or very slow to convert **1** to AHAs and mainly **4**. Reaction with Al^{III} and Cr^{III} halide catalysts is restricted to acetalization, like HCl. Nevertheless, when contacting the two metal halides with tetroses instead of dimeric GA **1**, MMHB **9** was analyzed to be in the range of 12% yield after 1 h.[22]

In conclusion, Sn halides are unique in converting the smallest sugar molecule glycolaldehyde into AHAs, preferably to MMHB **9** in methanol, and Brønsted acids and other Lewis acid catalysts mainly form diacetal GADMA **4**.

Proposal of the Reaction Pathway to MMHB. Considering the above study on the occurrence of GA in methanol and the earlier proposed reaction scheme for the conversion of tetroses to four-carbon AHAs,[22] a reaction

Scheme 3. Proposed Cascade of Glycolaldehyde (dimeric form 1) to MMHB 9 in CH_3OH in the Presence of Sn Halides

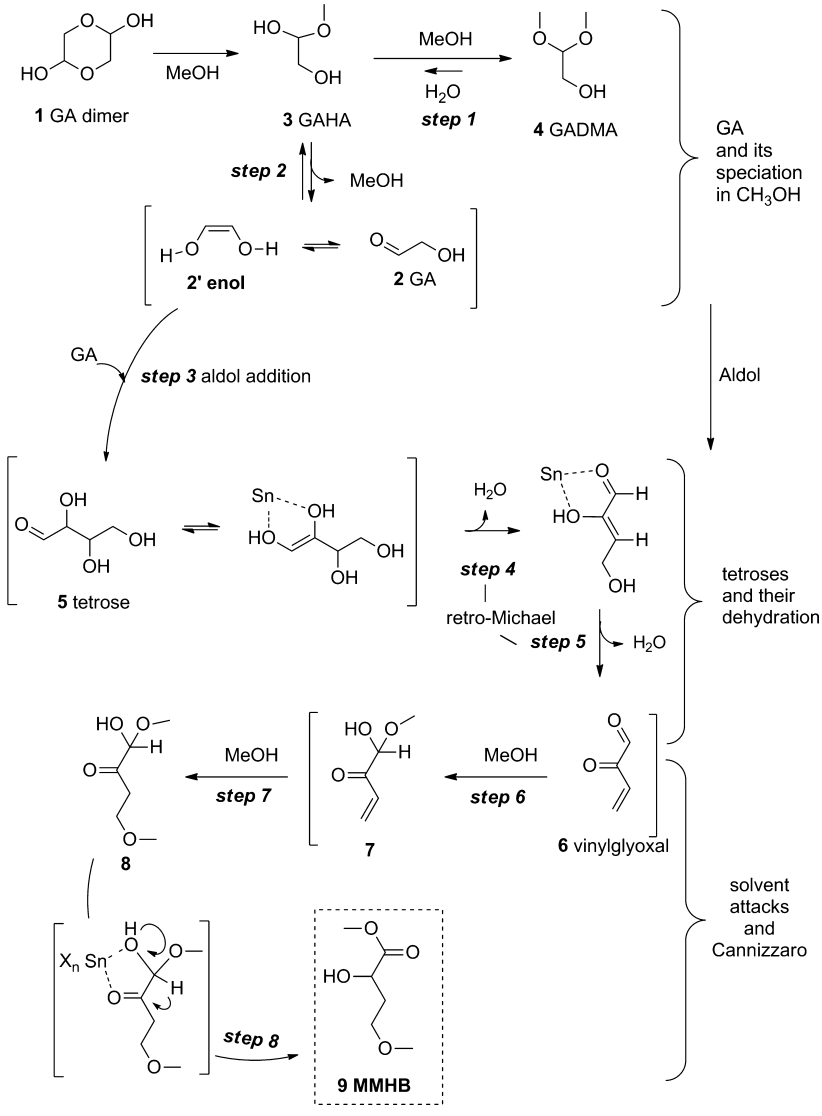

dx.doi.org/10.1021/cs400298n | ACS Catal. 2013, 3, 1786−1800

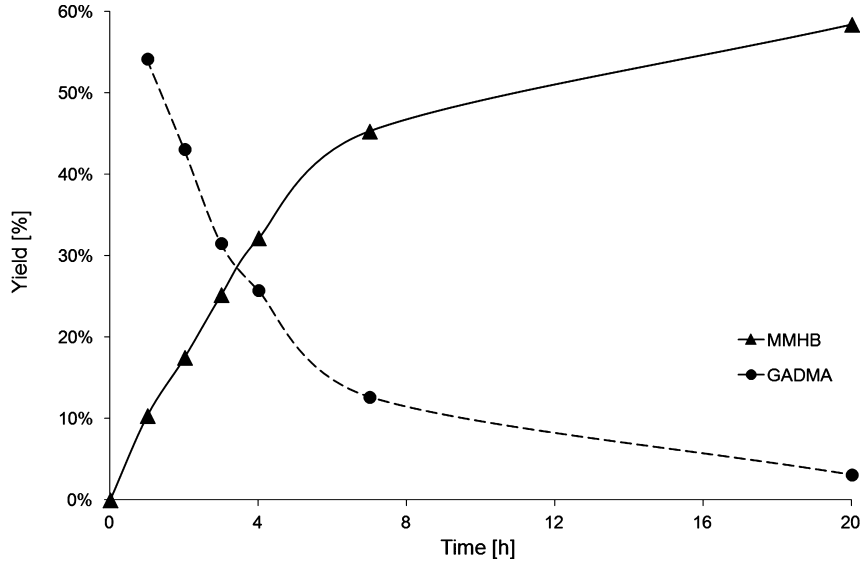

Figure 2. Kinetic plot of the reaction with $SnCl_4 \cdot 5H_2O$ in the conditions of Table 1, footnote a.

pathway for the conversion of **1** to MMHB **9** with Sn halides is postulated in Scheme 3. Acetalization in methanol rapidly converts **1** quantitatively into **4** at elevated temperature and in the presence of the Sn catalyst. To ascertain this, a reaction at 363 K with $SnCl_2 \cdot 2H_2O$ was quenched after 5 min in ice, and both GC and ^{1}H NMR pointed to formation of **4** in yields of 84 and 95% (±5%), respectively. In fact, glycolaldehyde dimethylacetal **4** may be regarded as the starting point under the reaction conditions, which is fully in line with the first points in the kinetic plot in Figure 2.

To be able to perform a Sn halide-based aldol reaction step, free GA **2** and its enol **2′** should be available. Therefore, step 1 in Scheme 3 considers the hydrolysis of **4** into the hemiacetal **3**. This step obviously requires the presence of water. Water can be traced back to three different sources in the reaction: (i) Sn halide is used in its hydrate form; (ii) water is also formed in the reaction network, considering the two necessary retro-Michael dehydrations of the tetrose en route to an AHA,[22] and (iii) when no special precautions are taken, methanol contains small percentages of water, which is easily detected by ^{1}H NMR. Acetalization is reversible and usually catalyzed by acid catalysts.[53] Similar to the hydrolysis of **4** to **3** (step 1), the latter is in equilibrium with free GA **2** and **2′**, via the loss of another methanol (step 2 in Scheme 3). Formally, this step can also be written as a hydrolysis followed by dehydration. The enol species **2′** is capable of attacking a free GA molecule **2** to form a tetrose **5** via aldol addition. With Sn halides in alcoholic media, the base-catalyzed aldol mechanism[41,42,54] is excluded, since the medium is neutral to acidic, depending on the level of methanolysis/hydrolysis of the chloride ligands at the Sn Lewis acidic center. Furthermore, the reported enamine aldol mechanism[51,55] is excluded due to lack of amines. This leaves us with two possibilities: a Lewis acid Sn-catalyzed aldol, as in the origin of life approach with Zn^{II} by Kofoed et al.,[55] or a Brønsted acidic aldol addition. The latter may be tentatively excluded because a reaction of 1 with HCl forms only **4**, but this will be discussed later.

Following the formation of the tetrose **5**, two retro-Michael dehydration steps[56] follow (step 4 and 5). Since Sn easily coordinates to entities with multiple −OH or =O bonds (such as sugars) due to its strong Lewis acid character,[57,58] such dehydration may formally be written, as if catalyzed by the Sn center. A similar reaction mechanism was proposed for the dehydration of dihydroxyacetone to pyruvic aldehyde with Sn halides.[59] Even when incorporated in *β*-zeolites, Sn centers were found capable of coordinating multiple oxygen groups of sugars, and this proves, for instance, useful in the isomerization of glucose to fructose[60] via a hydride transfer mechanism[61,62] and the epimerization of sugar borate complexes.[63]

Scheme 3 suggests the formation of a reactive intermediate vinyl glyoxal **6** as a result of the dehydration steps. This unsaturated molecule is prone to be attacked by nucleophiles on its conjugated vinyl group according to a 1,4-addition[64,65] and on its terminal carbonyl via acetalization. Acetalization, depicted as step 6, is fast in the reaction conditions and leads to hemiacetal **7**. Subsequent alcohol attack on the vinyl group, presented as step 7 (in Scheme 3), follows a formal 1,4-nucleophilic (Michael) addition on *α*,*β*-unsaturated carbonyls[65] and leads to the formation of the hemiacetal of 4-methoxy-ethylglyoxal (**8**, Scheme 3). This molecule has been encountered in high amounts as an intermediate when reacting tetrose sugars with tin halides.[22] Earlier work on tetroses showed that pure Brønsted acidic catalysts are also able to accelerate the conversion of tetroses to the hemiacetal **8**, but then eventually lead to the formation of a dimethyl acetal of **8** (not shown). This further proves that the cascade of retro-Michael dehydrations, hemiacetalization and 1,4-addition is also catalyzed by Brønsted acids, but interestingly, not the final further conversion of **8** to MMHB **9**.[22] This final step 8 is a formal intramolecular Cannizzaro reaction, which shifts the proton of the aldehyde (here in hemiacetal form) of **8** via hydride transfer from the terminal carbon to the *α*-carbon, with formation of *α*-hydroxy acid ester MMHB **9** as the final result. This type of reaction occurs only with Sn Lewis acid sites under mild conditions and is, for instance, also responsible for the conversion of pyruvic aldehyde into lactates.[1,5,66,67]

As deduced from Table 1, the overall cascade transformation of **1** into **9** in methanol is much slower than the reaction with tetroses **5**−**9** (steps 4−8). This indicates that the rate-determining step (rds) of the cascade occurs in steps 1−3. Gaining insight into the rds of a cascade reaction is very instructive to assess the foremost catalytic needs. Mechanistic

dx.doi.org/10.1021/cs400298n | *ACS Catal.* 2013, 3, 1786−1800

insight may suggest rate improvements by better balancing the required multiple active sites.[5,68,69] Two in situ NMR studies were therefore performed to provide evidence for the proposed reaction scheme, one for the conversion of a tetrose **5** and one with glycolaldehyde as substrate.

In Situ ^{13}C NMR Study in CH_3OH: GA vs Tetroses. The rate-determining step in the conversion of tetroses (**5** in Scheme 3) to MMHB (**9** in Scheme 3) can be deduced from the in situ ^{13}C NMR series shown in Figure 3, iii–v. The first

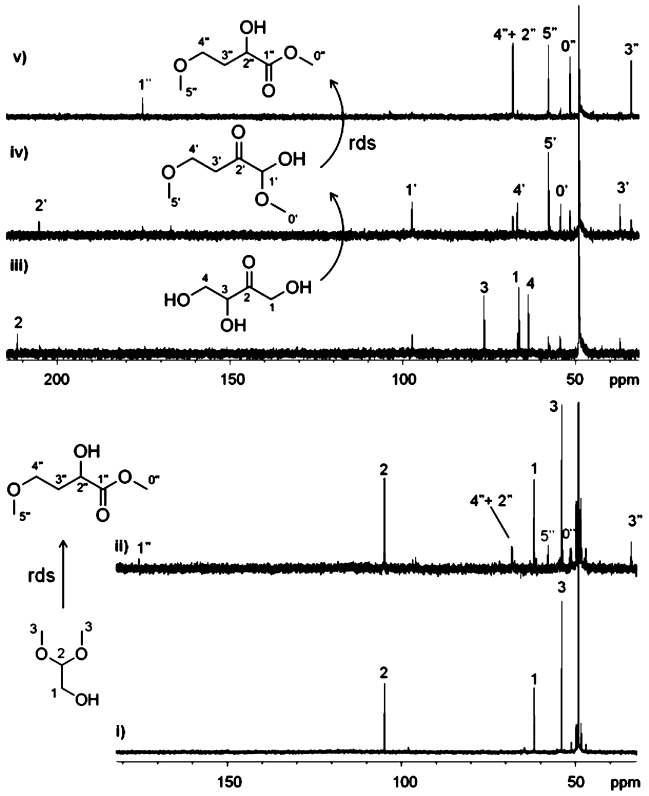

Figure 3. In situ ^{13}C NMR study with GA dimer **1** (i, ii) and erythrulose (iii–v) in contact with $Sn^{IV}\cdot 5H_2O$ in CH_3OH, at 333 K: (i) 10 min, GADMA; (ii) 13 h later, presence of GADMA **4** and MMHB **9**; (iii) 10 min at 298 K, mainly tetrose; (iv) 10 min at 333 K, formation of the hemiacetal of 4-methoxyethylglyoxal **8**; (v) 100 min at 333 K, formation of MMHB **9**.

spectrum is obtained directly after mixing the tetrose **5** solution with the Sn halide and shows mainly the four characteristic peaks of erythrulose (Figure 3iii, signals 1–4). One can also study the aldose erythrose, rendering the same catalytic results,[22] but its starting ^{13}C NMR spectrum is less straightforward.[70] Quickly, after 10 min at 333 K, signals 0–4 vanished in favor of 6 new ones (Figure 3iv, signals 0′–5′), which are indicative of the presence of the hemiacetal of 4-methoxyethylglyoxal (**8** in Scheme 3, earlier confirmed with chemical ionization mass spectrometry[22]). After longer times, namely, 100 min at 333 K, six new ^{13}C NMR signals show the presence of MMHB **9** (Figure 3v, signals 0″–5″). The in situ time profile agrees with the intermediate accumulation of **8** and hereby proves that the slowest step in the conversion of **5** to **9** is the final Cannizzaro (step 8 in Scheme 3).

However, when contacting **1** in the same reaction conditions, the first spectra display the acetal GADMA **4** (Figure 3i, signals 1–3), and over prolonged reaction times, its signals slowly turned in favor of **9** (Figure 3ii, signals 0″–5″) without visibly passing through the hemiacetal of GA **3** or the hemiacetal of 4-methoxyethylglyoxal **8**. This suggests that the rate-determining step of the cascade reaction is not the Lewis acid-catalyzed Cannizzaro, but step 1, the hydrolysis of **4** to **3**. Indeed, if, for instance, step 2 were the slowest step, the hemiacetal **3** should be clearly visible in the NMR spectra, which is not the case.

In conclusion, in contrast with the conversion of tetroses to AHAs, the overall rate of MMHB formation from **1** is determined by the Brønsted acid-catalyzed hydrolysis of acetal **4**. This insight implies (1) an optimal balance between Lewis and Brønsted acidity to obtain a maximum overall rate and (2) a well-thought choice of the reaction solvent and the presence of water as they determine the occurrence of GA. To corroborate these hypotheses, several variations both at the level of the catalyst (1), and of the solvent (2) are put forward in a new series of experiments in the next paragraphs.

Mechanistic Implications at the Level of the Catalyst. The interplay between the Lewis and Brønsted acidity derived from the Sn halide salts in the reaction medium is thought to be crucial to the overall rate of the cascade. On the basis of the aforementioned results, it seems that step 1 in Scheme 3 (viz., the Brønsted acid catalyzed hydrolysis of acetal **4**) determines the overall rate. Reaction of 1 with 20 mol % HCl yields no **9**, but shows formation of only **4**; the initially suggested Brønsted acid-catalyzed enolate mechanism for the aldol addition is thus not a major pathway here (entries 2, 3 in Table 1). The observation proves that condensation of two GA molecules requires the action of the Lewis acidic Sn (see step 3). Although not rate-limiting, this Lewis acid-catalyzed addition is crucial for the feasibility of the cascade, which leads to the formation of **9**. Although the main occurrence of GA in methanol at room temperature is **3**, when Brønsted acidity is present, **4** dominates in a dynamic equilibrium. The same is true in the presence of Sn halides, but the difference here is that the slightest conversion of **4** to **3** and further to free GA **2** and its enol **2′** allows aldol addition to a tetrose **5** under the action of Lewis acidic Sn, with rapid subsequent conversion of **5** into AHA esters. It is therefore very likely that a Lewis acid Sn-catalyzed aldol reaction via the enolate mechanism is occurring, as was postulated for Zn^{II} by Kofoed et al. in their origin of life approach. HCl, Al^{III}, and Cr^{III} halides, for instance, appear unable to efficiently catalyze the aldol coupling, and the reaction its trapped in the production of acetal **4**. Even though these halides are able to fully convert tetrose feedstock in 1 h,[22] their inefficient aldol traps the reaction with GA in acetal **4**.

In conclusion, next to its role in the 1,2-hydride shift (Cannizzaro, converting **8** to **9**), Lewis acid tin is also essential in catalyzing the aldol reaction of **2** to **5**. However, because the rate of the cascade is determined by the hydrolysis of acetal **4**, the balance between Brønsted and Lewis acidity is key to understanding and directing the cascade reaction of **1** to **9** toward a high rate and selectivity and, thus, a high-volume productivity.

A closer look at the properties of $Sn^{IV}Cl_4\cdot 5H_2O$ learns that in water, hydrolysis to $Sn^{IV}(OH)_4$ is complete and fast with release of 4 HCl per Sn, lowering the pH of water. The same was witnessed for $Sn^{II}Cl_2\cdot 2H_2O$. When the chloride ligands of Sn^{IV} are neutralized (for instance with NaOH), the Sn^{IV} centers tend to condense, and precipitation is swift, pointing to the formation of tin (hydr)oxides. In methanol, traces of water could hydrolyze chloride ligands, but a methanolysis with formation of HCl is possible, as well. Neutralization of the

dx.doi.org/10.1021/cs400298n | ACS Catal. 2013, 3, 1786–1800

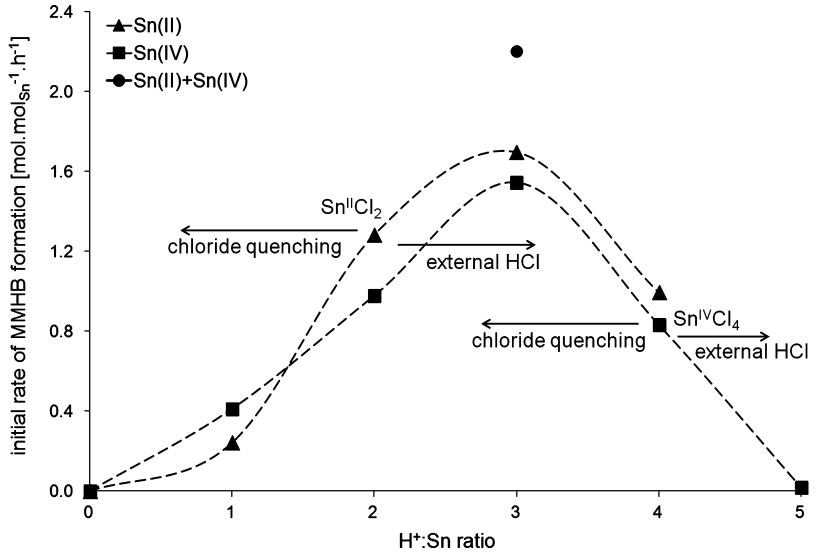

Figure 4. Initial rate of MMHB **9** formation in function of H^+/Sn ratio. Variation of the ratios obtained for both Sn^{II} and Sn^{IV} by quenching Cl^- with an anion exchange resin (OH^- form) or by adding extra HCl. The rate obtained by an equimolar mixture of $SnCl_2$ and $SnCl_4$ is presented with the solid circle (●). Rates were measured in the linear part of reactions at 363 K with 1.25 M GA in the presence of 5 mol % of Sn in CH_3OH (as demonstrated in Figure 5).

generated acidity stoichiometrically in methanol with NaOH also leads to cloudy suspensions, but no heavy precipitate, as in water, was noticed. Under the nonneutralizing reaction conditions in methanol, it is difficult to determine the exact grade of methanolysis (and hydrolysis). Nevertheless, use of tin chlorides in methanol delivers Brønsted acidity in the form of HCl to the reaction medium, next to Lewis acid Sn centers. In the envisioned cascade reaction in Scheme 3, where multiple steps are catalyzed by either Brønsted acids, Lewis acids, or both, the intrinsic balance between both types of acid sites is crucially governed by the choice of halide and its ease of release.

Different kinetic experiments were undertaken with varying Brønsted and Lewis acid contents to assess the influence of different Brønsted vs Lewis acid ratios on the overall rate of reaction. For probing higher ratios, external HCl is added, whereas controlled assessment of lower ratios is obtained by partial quenching of the HCl formed from the Sn halide by methanolysis (and hydrolysis). Whereas the addition of HCl is straightforward, quenching of HCl is carried out with a quaternary ammonium anion exchange resin, exchanged in its OH^- form. This resin is added at the start of the reaction in precise amounts (its capacity was measured by titration) so as to capture the desired amount of Cl^- and to quench H^+ with the released OH^- equivalent. Test titration of such a resin with HCl in methanol proved that the ion exchange process is rapid, and the resin kept the medium free of acid until its point of saturation was reached. Thus, depending on the amount of resin or HCl added, different ratios of H^+/Sn are attained for both Sn^{II} and Sn^{IV}. Their influence on the rate of MMHB formation is plotted in Figure 4.

The highest formation rate of **9** is clearly observed for a H^+/Sn ratio of 3, and this value is surprisingly irrespective of the oxidation state of the Sn salt. In other words, the highest initial rate is noticed either when $SnCl_2$ is combined with 1 extra equiv of HCl or by quenching 1 equiv of HCl with the resin, when $SnCl_4$ was used. It is noteworthy that the overall rate of the cascade (at a certain temperature) can thus be maximized, simply by adding 1 equiv of HCl per Sn^{II} site to the reaction. Considering the rate-determining hydrolysis of **4** in the network, a ratio of 3:1 H^+/Sn indeed makes sense. A reaction with only HCl (as in entry 2, Table 1) simulates an infinite H^+/Sn ratio (on the *x*-axis in Figure 4), for which **9** is not formed because of a lack of aldolization (Sn) capacity. According to the reaction scheme, this zero rate indeed derives from the fact that, although the hydrolysis of **4** to **3** can be fast as a result of the presence of Brønsted acidity, the slowest step is now found in the aldol addition of **2** to **5**, which does not pull GADMA **4** away from the equilibrium. Figure 4 thus shows the importance of a balanced catalytic system with a preferred H^+/Sn ratio of 3.

To further corroborate this "magic" number, a reaction was performed with an equimolar mix of $SnCl_2$ and $SnCl_4$, which should lead to the ideal H^+/Sn ratio of 3. The result is plotted in Figure 4 (solid circle). Under these conditions, it represents the highest rate measured in methanol, proving once more that subtle tuning of the H^+/Sn ratio is a prerequisite to rapidly convert **1** to **9**. To witness a more efficient use of Sn, a reaction with only 1 mol % of such Sn^{II+IV} mixture was performed, and an initial rate of 3.4 mol_{MMHB} mol_{Sn}^{-1} h^{-1} was witnessed and yielded 50% of MMHB at full conversion. Note that these mechanistic insights are very instructive for future development of more sustainable heterogeneous Sn catalysts:[58,67,71−74] not only is the amount of Sn important, but also the presence of some Brønsted acidity is required to form AHAs at a maximum rate. A recent example, in which such subtle catalytic fine-tuning (by, for instance, spatial compartmentalization of the active sites) led to very high turnover frequencies (based on Sn), was found in the carbon−silica composite catalyst design described by de Clippel[75] and Dusselier et al.[5] for the formation of lactate esters from trioses and hexoses.

Consequence of the Addition of Water on the Rate. According to the enolate mechanism of the aldol addition, the solvent and the occurrence of GA indisputably influence the reaction rate and its selectivity. As seen above, the dominant form of GA under reaction conditions in methanol is **4**, whereas the species of interest for aldol addition is free aldehyde **2** and its enolate **2′**. Indeed, although the equilibrium situation in the upper part of Scheme 3 is in favor of **4**, the reaction network is dynamic as long as an appropriate Lewis acid catalyst is present.

dx.doi.org/10.1021/cs400298n | *ACS Catal.* 2013, 3, 1786−1800

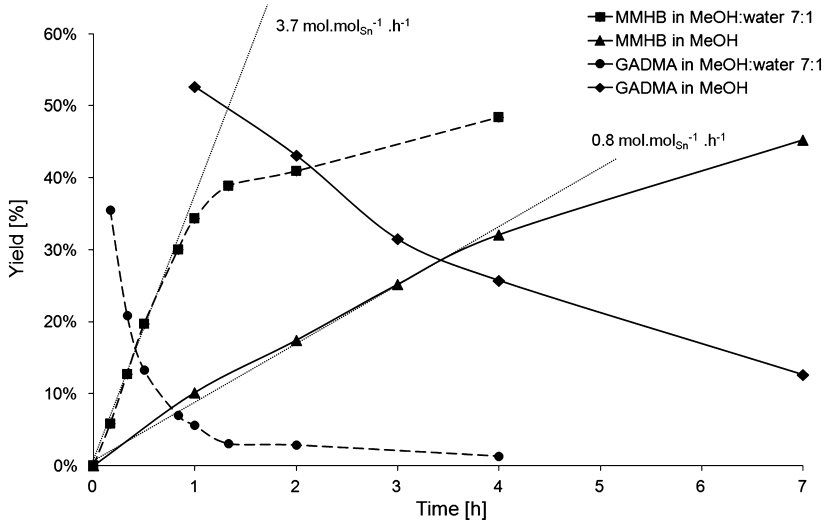

Figure 5. Kinetic plot for the conversion of 1.25 M GA in MMHB (**9**) catalyzed by 5 mol % of $SnCl_4 \cdot 5H_2O$ at 363 K in methanol (solid line) and in a methanol/water mixture (7:1 volume ratio) (dashed line).

Moreover, considering the rate-determining hydrolysis step **1** (or in other words, as the equilibrium favors **4**) in the overall cascade, the addition of some aliquots of water should greatly affect the overall reaction rate (or in other words, shift the equilibrium). Figure 5 presents the kinetic plots of a reaction carried out in either methanol or a mixture of 7:1 (v:v) methanol to water. From these plots, the initial turnover frequency (TOF) to convert GA dimer **1** to **9** was calculated, and it appears that the rate is, indeed, more than 4.5 times higher in the presence of water: namely, 3.7 vs 0.8 mol mol_{Sn}^{-1} h^{-1}. This value shows that Sn turns over GA at least 7.4 times every hour, which corresponds to a high productivity of 34 g_{MMHB} L^{-1} h^{-1} (first hour) in the concentrated solution. The superior rate achieved as a result of adding small amounts of water was seen as well with in situ ^{13}C NMR (see Supporting Information Figure S3). The spectral sequence demonstrates the same profiles as in Figure 3i−ii, but in a much shorter time frame: after 200 min at 333 K, all major signals encountered in the NMR spectrum belong to **9**.

Other ratios of methanol to water were screened, as well, and it was found that a ratio of 10:1 is sufficient to drastically accelerate the reaction with respect to pure methanol (kinetic plot, see Supporting Information Figure S4). The effect of water is also apparent in the data of Table 2, which displays MMHB yields after 1 h of reaction in different solvents. Comparing entry 1 with entries 2 and 3 shows that, indeed, the MMHB yield is more than tripled as a result of the addition of water in the first hour. There is an optimum amount of water required to speed up the reaction, since a rate decrease was observed after adding too much water (a 1:1 volume ratio). The latter is likely caused by the formation of insoluble Sn (hydr)oxide species, as ascertained by precipitate formation upon visual inspection. Since the reaction in water-containing methanol is very fast, the temperature dependence of this cascade reaction was assessed. At a volume ratio of methanol to water of 7:1, the overall activation energy for formation of **9** from **1** corresponds to a value of 73 kJ·mol^{-1} (Arrhenius plot, see Supporting Information Figure S5). The requirement of water to speed up the overall reaction can be seen as an advantage because GA is usually provided in aqueous solutions; for instance, via its recently reported separation from biomass pyrolysis oils.[35] There is thus no need to perform expensive drying to remove all the water from such GA solutions. Methanol should simply be added to fairly concentrated aqueous solutions of GA if MMHB is desired.

Table 2. Effect of Solvent Changes (other alcohols and presence of water) on the Yield (obtained after 1h) to the Corresponding AHAs

entry	solvent (v:v)	MMHB (%)[a]	MVG (%)[a]	ratio[b]
1	CH_3OH	10	<1	
2	CH_3OH/H_2O 7:1	34	2	17
3	CH_3OH/H_2O 10:1	35	2	17
4[c]	EtOH	26[c]	5[c]	5.7
5[d]	IPA	15[d]	22[d]	0.7

[a]MMHB yields, 1 h at 363 K using 1.25 M GA with 5 mol % $SnCl_4 \cdot 5H_2O$. [b]Molar ratio of alkyl-4-alkoxy-2-hydroxy-butanoate/alkyl vinyl glycolate. [c]Reaction leads to ethyl-4-ethoxy-2-hydroxybutanoate (EEHB) and ethyl vinyl glycolate (EVG). [d]Reaction leads to isopropyl-4-isopropoxy-2-hydroxybutanoate (IIHB) and isopropyl vinyl glycolate (IVG). For identification, see Supporting Information Figures S6 and S7.

Reaction in Other Solvent Media: Formation of Vinyl Glycolate and Its Esters. Entries 4 and 5 in Table 2 show the (nonoptimized) reactions carried out in ethanol and isopropyl alcohol (IPA), respectively. In ethanol, the yield to the corresponding ethyl vinyl glycolate (EVG) is noticeable whereas the corresponding MVG formation in methanol barely is; however, ethyl-4-ethoxy-2-hydroxybutanoate (EEHB) remains the major product. The ratio of EEHB to EVG is around 6, whereas in methanol, the corresponding MMHB to MVG ratio is usually above 15 (entries 1, 2 in Table 2 and 6, 8 in Table 1). Use of IPA shows the reverse chemoselectivity with a preference for vinyl glycolate ester (IVG) formation; the more sterically demanding alcohol indeed led to ∼22% of isopropyl vinyl glycolate (IVG) in 1 h of reaction time, in addition to 15% of isopropyl-4-isopropoxy-2-hydroxybutanoate (IIHB). The corresponding ratio of IIHB to IVG is thus clearly <1. Such reverse selectivity pattern is in agreement with earlier reported conversion of tetroses to AHAs.[22]

To understand the shift in product selectivity upon using different solvents, the proposed reaction scheme is drawn in

dx.doi.org/10.1021/cs400298n | ACS Catal. 2013, 3, 1786−1800

Scheme 4. Proposed Reaction of GA in IPA or Nonalcoholic Media with Sn Leading to Vinyl Glycolic Acid (VG) or Its Isopropyl Ester (IVG), 2,4-Dihydroxybutanoic Acid (2,4-DHB) and α-Hydroxy-γ-butyrolactone (HBL)

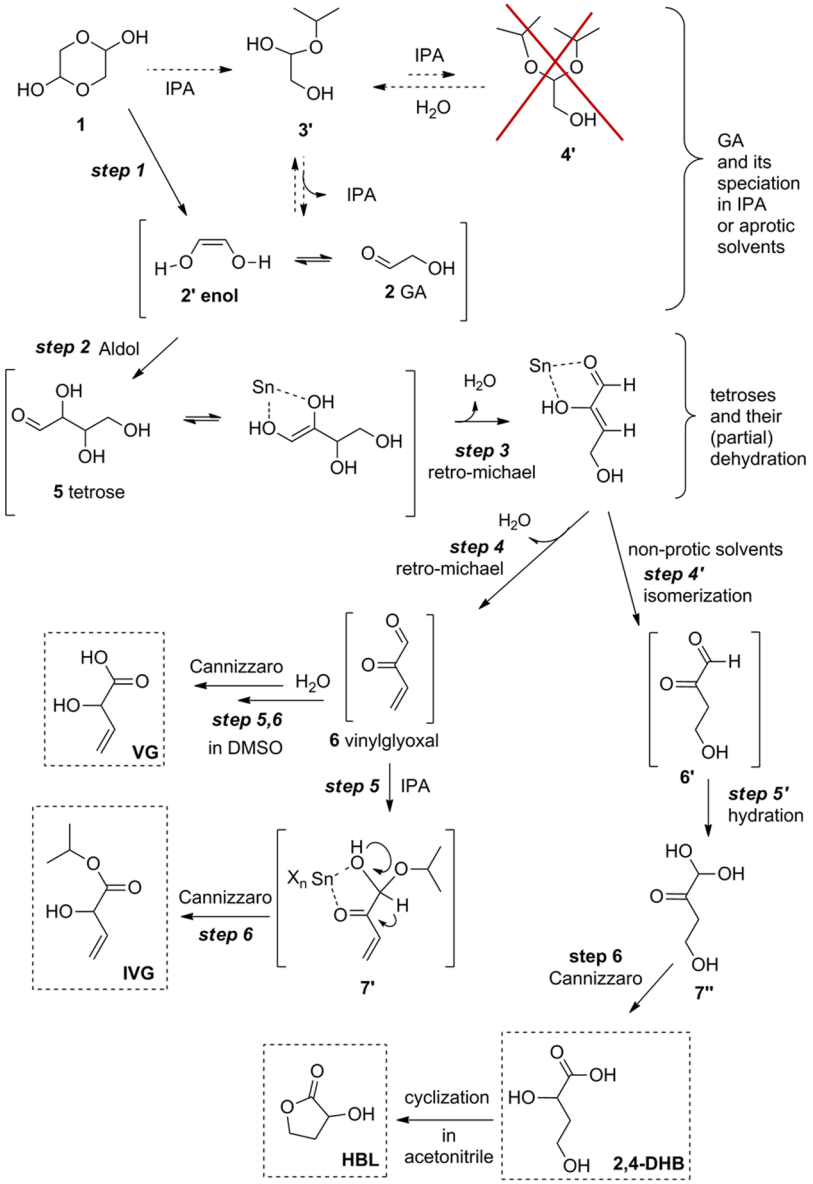

more detail in the case of IVG formation in IPA (Scheme 4). Comparison of this scheme with Scheme 3 reveals a major difference at the level of the occurrence of GA. ^{13}C NMR and GC/MS witnessed no formation of the di-isopropyl acetal **4′**, which appears unfavorable for steric and electronic reasons. Therefore, it is suggested that the reaction equilibrium in IPA is more in favor of the hemiacetal **3′** and free GA (**2** and **2′**). A kinetic experiment in IPA (see Supporting Information, Figure S8) for the formation of AHA esters (the sum of IVG and IIHB) attained a very fast initial rate of about 16 mol_{AHA} mol_{Sn}^{-1} h^{-1} in its very short linear part and reaches ~40% of AHA esters already after 1.5 h of reaction. This reaction runs very fast when compared with the aforementioned rates in methanol because GA is less protected in (hemi)acetals, and thus, more available for aldolization. Once the aldol reaction has occurred with formation of tetrose **5**, little difference is to be expected between the reaction rates in isopropyl alcohol and methanol. The product selectivity, though, is significantly different, and this difference is easily explained in the following course of the cascade reaction, in accordance with Scheme 4.

Indeed, once the vinyl glyoxal **6** and its isopropyl hemiacetal **7′** is formed from the tetrose **5** as a result of two retro-Michael dehydration steps, the unique selectivity pattern of IPA becomes apparent: isopropyl alcohol, a more sterically hindered and less nucleophilic alcohol, is less reactive toward the 1,4-addition on the vinyl group than, for example, methanol, whereas the rate of the intramolecular Cannizzaro, a 1,2-hydride shift catalyzed by the Lewis acid Sn center, is not greatly affected by variation of the alcoholate. Once the hydride shift (step 6 in Scheme 4) proceeds, an α-hydroxy group is formed on the second carbon, and the 1,4-addition on the vinyl can thus no longer proceed because of a lack of conjugation. IVG is thus the preferred product in isopropyl alcohol, and MMHB is the dominant product in methanol. The 1,4-nucleophilic addition is only slightly hindered in ethanol, when compared with the intramolecular Cannizzaro, and significantly more of the ethyl ether compound (EEHB) is formed (EEHB/

dx.doi.org/10.1021/cs400298n | ACS Catal. 2013, 3, 1786−1800

EVG is 7:1). The rate in ethanol is also significantly higher than in methanol, but lower than in isopropyl alcohol; its value corresponds to 4 mol_{AHA} mol_{Sn}^{-1} h^{-1} (from Supporting Information Figure S8). This is, of course, linked to the occurrence of GA in ethanol, in which the formation of glycolaldehyde diethyl acetal was noticed. Its formation was, however, less pronounced than GADMA **4** in methanol, implying a faster reaction in ethanol.

In addition to the mechanistic findings in alcohols, reactions in nonalcoholic polar media were screened, as well (dimethyl sulfoxide (DMSO) and acetonitrile). Interestingly, a selectivity pattern similar to that in IPA was encountered in DMSO, with vinyl glycol acid as the dominant product. The molar ratio of 2,4-dihydroxybutanoic acid (2,4-DHB) to VG is around 0.3, according to NMR analysis on the crude mixture. Scheme 4 also summarizes the different reactions leading to VG and 2,4-DHB in nonalcoholic solvents. VG formation follows the same pathway as formation of IVG and MVG, with water as the nucleophile, whereas we found that the formation of 2,4-DHB surprisingly does not follow the analogue pathway of MMHB synthesis in methanol (or IIHB in IPA, not shown). To unravel what happens in such a solvent, a reaction at 333 K with 20 mol % $SnCl_4{\cdot}5H_2O$ was followed in situ with ^{13}C NMR in DMSO. By comparing the AHA formation rate with that of a similar in situ reaction in methanol (see the spectra in Figure 3), a very fast formation of VG in DMSO was noticed: VG is already formed after 1 h of reaction, whereas 12 h is required to form MMHB in MeOH under comparable in situ circumstances. This rate increase obviously originates from the high availability of free GA because acetal formation in DMSO does not occur. The evolving spectral sequence and time scale is shown in Figure 6, as well as the final result of an in situ ^{13}C NMR study

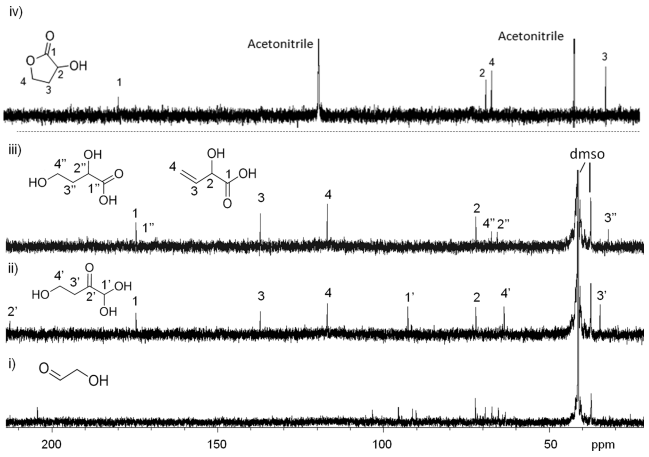

Figure 6. (i–iii) In situ ^{13}C NMR in DMSO: 1.25 M GA and 20 mol % of $SnCl_4{\cdot}5H_2O$ evolving in time at 333 K (10, 110, and 700 min, respectively, after mixing). (iv) Final spectrum of the in situ ^{13}C NMR study in acetonitrile (1.25 M GA, 2 h at 333 K, 50 mol % of $SnCl_4{\cdot}5H_2O$, acetonitrile/H_2O = 7:1).

in acetonitrile. Spectrum i of Figure 6 shows the signals of the products encountered in DMSO after 10 min at 333 K. Dimer **1** is likely completely converted to free GA and its enolate,[48,49] and GA hydrates and possibly tetroses signals are also apparent in the complex spectrum. The spectrum after 110 min, Figure 6ii, is easier to understand because it shows chemical shifts due to VG (1 to 4) and the hydrate of 4-hydroxyethylglyoxal (signals 1′–4′, structure **7′** in Scheme 4.) The product mixture after 700 min contains mainly VG (signals 1–4) next to some 2,4-DHB (signals 1″–4″).

As seen in Scheme 4, dimer **1** is thus easily converted to free GA **2** (and its enolate **2′** and some hydrates) in DMSO or acetonitrile. Aldolization of GA under action of Sn produces tetroses, which are prone to undergo two retro-Michael dehydrations to form the reactive vinyl glyoxal **6**. In DMSO, the double bond of **6** is mostly preserved, and since traces of water are the only nucleophile present, a hydrate of vinyl glyoxal is formed, which transforms into VG as a consequence of the tin-catalyzed internal Cannizzaro reaction. Water in DMSO apparently does not favor attack on the vinyl because a 1,2-hydride shift of the hydrate is faster. To confirm VG as the main product after reaction in DMSO (as seen, for instance, in Figure 6iii), such a mixture was diluted in methanol and allowed to react at 363 K. In this way, esterification of VG to MVG in methanol with the assistance of the Sn-released HCl could be monitored by GC/MS analysis; such MVG formation may be interpreted as an indirect proof of VG formation in DMSO.

Although less pronounced, a competitive pathway was encountered: after the first retro-Michael (step 3, Scheme 4), an isomerization (step 4′, Scheme 4) can take place, forming 4-hydroxyethylglyoxal **6′**, which is easily hydrated to **7′′**. This compound, **7′′**, was analyzed with in situ ^{13}C NMR, as seen in spectrum ii of Figure 6. Species **7′′** subsequently transforms into AHA 2,4-DHB (as seen in Figure 6iii), according to the Sn catalyzed intramolecular Cannizzaro reaction. A closer look at 2,4-DHB reveals that the molecule should be prone to intramolecular esterification, especially in the presence of some free HCl from the Sn halide, leading to a cyclic four-carbon AHA ester: α-hydroxy-γ-butyrolactone (HBL). In fact, HBL is the dominant product formed in acetonitrile, as witnessed by the ^{13}C NMR spectrum iv in Figure 6. Its formation was also confirmed with GC/MS.

Incorporation of VG in Poly(L-lactic acid) (PLLA). After successfully converting glycolaldehyde in various types of AHAs (and their esters), such as MMHB, MVG, 2,4-DHB, and HBL, we were interested in their ability as bioderived building blocks for polymer chemistry. A conceptual proof of their value is illustrated with the incorporation of VG into PLLA. Because one of the shortfalls of traditional PLLA is its lack of reactive side groups,[8,19,76] the vinyl group of the VG monomer potentially offers a creative solution to this problem by its cocondensation with lactic acid. Such a copolymerization approach has been proposed earlier for different monomers by using functional lactide derivatives for ring-opening polymerization.[77−80] The incorporation of VG in PLLA has not been reported, but it would offer a tremendous versatile side group in PLLA, which could be further modified easily with elegant organic chemistry, such as thiol-ene protocols.[81−83] For instance, if the vinyl is modified with a hydrophilic moiety, another drawback of PLLA (namely, a too-pronounced hydrophobicity) can be tackled at once.

To incorporate vinyl glycolic acid (VG) into PLLA, MVG was hydrolyzed (see Supporting Information Figures S10, S11) and mixed with L-lactic acid before polycondensation. The copolymerization was performed via azeotropic distillation for water removal, according to Kim et al.,[47] in the presence of $SnCl_2{\cdot}2H_2O$ catalyst in *p*-xylene. Not only are such tin halide salts thus capable of producing the monomers from bioderived GA (this work) and tetroses,[15] they are also known catalysts for the synthesis of PLA via polycondensation. After precipitation

of the polymer in cold MeOH, in which nonreacted monomers remain soluble, ^{1}H NMR (see Figure 7) and ^{13}C-APT-NMR

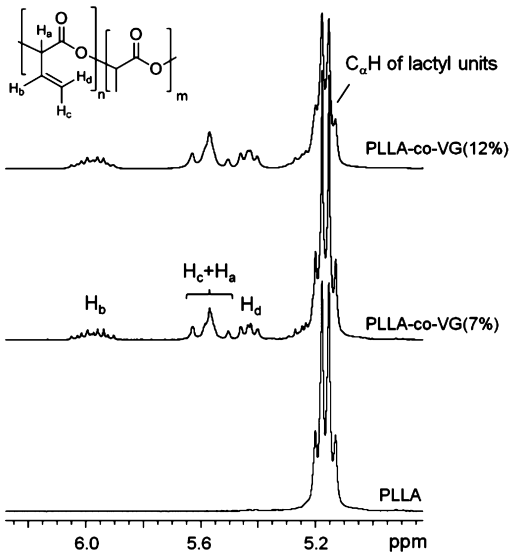

Figure 7. ^{1}H NMR of PLLA and PLLA-co-VG.

(see Supporting Information Figure S12) unambiguously proved the incorporation of the vinyl monomer into PLLA. The vinyl signals in Figure 7 (H_b, H_c, and H_d) as well as the proton of the α-carbon (H_a), to which the vinyl is attached, are found between 5.4 and 6.1 ppm. From the integration values of these ^{1}H NMR spectra, it was calculated that PLLA-co-VG with 7 and 12% of VG was successfully synthesized using different ratios of monomer in the procedure. Table 3 presents the

Table 3. Different Polyesters and Some of Their Properties

polymers[a]	M_n[b] (g mol^{-1})	Đ[c]	Contact Angle[d] (°)
PLLA	17 100	1.9	76.3 ± 0.4
PLLA-co-VG(7%)	14 500	1.7	
PLLA-co-VG(12%)	12 600	1.6	77.3 ± 2.5
Modified Polymers[e]	X_{vinyl} (%)[f]		
PLLA-co-VG(12%)-BM	>96		76.3 ± 2.4
PLLA-co-VG(12%)-TG	>98		66.7 ± 1.9

[a]Obtained via polycondensation. Value in brackets: mol % of VG units in copolymer. [b]Number averaged molecular weight via SEC, relative to polystyrene. [c]Dispersity. [d]Water contact angle. [e]Modified via radical thiol-ene with benzyl mercaptan (BM) and thioglycerol (TG). [f]Conversion of the vinyl group upon modification, via ^{1}H NMR.

molecular weight of benchmark PLLA (prepared in exactly the same manner) and the novel PLLA-co-VG polymers; the values are in the range of 12−17 000 g mol^{-1}, and the dispersities, Đ, range from 1.6 to 1.9 (SEC, see Supporting Information Figure S13), with the novel polymers being a little more uniform in chain length.

The thermal behavior of the novel polyesters was assessed, and the data are summarized in Figure 8. It appears that when more vinyl monomer is incorporated into PLLA, the polymer remains stable for a longer time and, hence, degrades at a higher temperature in the thermal gravimetric analysis (Figure 8A). For example, PLLA-co-VG (12%) was up to 75 K more stable with respect to the genuine PLLA polymer. Possibly, the high thermostability arises from temperature-induced cross-linking. Several differential scanning calorimetry (DSC)

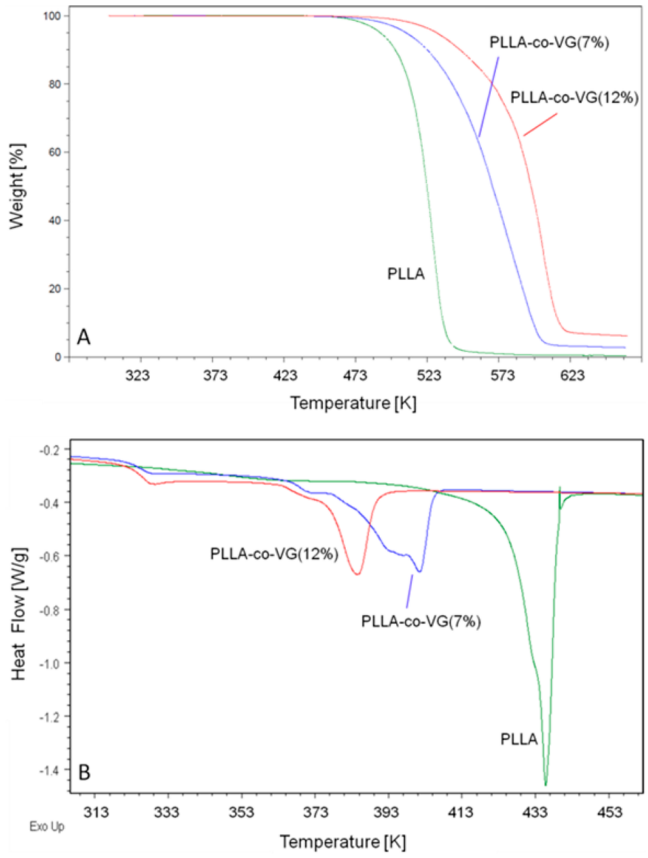

Figure 8. Thermal properties of PLLA and PLLA-co-VG (7 or 12%): (A) TGA (10 K/min, N_2); (B) analysis via differential scanning calorimetry (10 K/min, N_2, first heating cycle).

measurements seemed to confirm this (Supporting Information Figure S14). The thermograms in Figure 8B reveal that the vinyl-containing polyesters are less (semi)crystalline than the pure PLLA and melt at lower temperatures: the higher the vinyl incorporation, the lower the melting point. The glass transition for all three polymers was seen in the 323 to 333 K region. The lower melting temperatures combined with their prolonged thermal stability offers a broader window for thermal processing when compared with the traditional PLLA (for T_g and T_m, see Supporting Information Figure S14).

To prove the accessibility and reactivity of the vinyl moieties in the novel PLLA-co-VG (12%), UV-initiated radical thiol-ene derivatization experiments were performed with various thiols, such as benzyl mercaptan (BM) under mild conditions. The success and ease of this approach can be read from the vinyl conversions in Table 3 and in the corresponding ^{1}H NMR spectra in Supporting Information Figure S15. BM successfully reacted with the vinyl groups with an almost quantitative conversion. More interestingly, because reference PLLA is often considered too hydrophobic for certain applications, the ease of functionalization was utilized as a tool to enhance its hydrophilicity. Therefore, polar TG was chemically grafted onto the double bond, and the vinyl conversion was complete. Signals of the corresponding glycerol units were apparent in the polymer after precipitation in cold diethyl ether (Supporting Information Figure S15). In contrast to the reference PLA and the other (thiol-functionalized) PLLA-co-VG polyesters in this study, this TG-modified polymer did not precipitate in methanol, in line with its enhanced polarity. Static water

dx.doi.org/10.1021/cs400298n | ACS Catal. 2013, 3, 1786−1800

contact angle measurements on thin films, made via spin-coating, corroborated this hypothesis: although neither the incorporation of vinyl groups in PLLA nor the BM grafting influenced the contact angle greatly with respect to that of reference PLLA (76.3 ± 0.4°, in agreement with literature[84,85]), modification with the polar TG clearly caused a significant decrease of 10° of the water contact angle (see Table 3). These contact angles are visually presented in Figure 9 for PLLA and

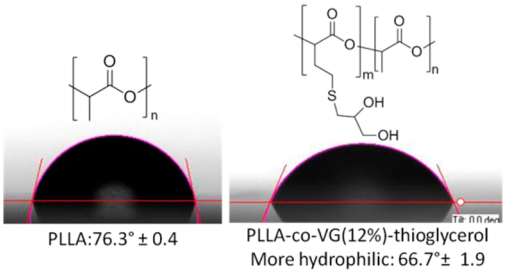

Figure 9. Structure of PLLA (left) and PLLA-co-VG(12%)-TG (right) and a representative droplet photograph.

PLLA-co-VG(12%)-TG (for more photos, see Supporting Information Figure S16). This example nicely illustrates that the novel four-carbon AHA monomers are easily incorporated in PLLA and truly offer added value in light of a controlled modification of the polymer functionality toward desired properties.

CONCLUSIONS

Glycolaldehyde, a main component of biomass-derived pyrolysis oils, was converted in one step into various four-carbon α-hydroxy acids and their esters. The choice of solvent mainly determines the product selectivity of the GA-to-AHA reaction. High yields of MMHB were, for instance, produced in methanol, whereas VG and 2,4-DHB are the dominant products in DMSO, and HBL is encountered in acetonitrile. IVG is the dominant ester in isopropyl alcohol. The one-pot reaction follows a complex cascade network in which both Brønsted and Lewis acid centers are playing a crucial role. Different intermediates and rate-determining steps were identified by in situ ^{13}C NMR. Sn halide salts are able to foresee both types of acid activities, and an optimal ratio of Brønsted to Lewis acid sites of ∼3 was determined in this work. Surprisingly, this ratio was irrespective of the oxidation state of the Sn ion. Lewis acid Sn is essential for the aldolization of GA to tetroses and the intramolecular Cannizzaro of intermediate glyoxals and their hemiacetals to the final AHAs (and their esters), HCl is likely responsible for fast hydrolysis of acetals to deprotect sufficient GA for aldolization and it is able to assist the retro-Michael dehydrations of tetroses into glyoxals and their 4-alkoxy ethers. Addition of some water to the reaction mixture also greatly improved the rate of reaction in line with the rate-determining GA (hemi)acetal hydrolysis in the overall cascade. The elucidation of this cascade reaction and its catalytic needs in terms of Lewis and Brønsted acidity should be inspiring to develop adequate heterogeneous catalysts for the title reaction.[5,59,68,72−74]

The value of such bioderived AHA monomers was illustrated for the first time by copolymerization of VG with L-lactic acid to obtain PLLA-based polyesters with vinyl side groups. The as-synthesized PLLA-co-VG polymers possess a larger thermal window for further processing compared with PLLA. Moreover, the presence of the vinyl group allows easy modification of the PLLA matrix to tune properties such as polarity; for instance, a polar PLLA-co-VG was easily synthesized by reacting the present vinyl groups with thioglycerol under UV irradiation according to thiol-ene chemistry.

ASSOCIATED CONTENT

Supporting Information

Additional in situ NMR studies (e.g., in methanol/water); analysis of chemicals and raw reaction mixtures (NMR); kinetic plots for reactions in IPA, ethanol, methanol, and methanol/water; and an activation energy plot are provided. A full characterization of the polymers (NMR, SEC, DSC (thermograms featuring T_g and T_m)) is given, as well as some of the representative static contact angle droplet photos. This information is available free of charge via the Internet at http://pubs.acs.org/.

AUTHOR INFORMATION

Corresponding Author

*E-mails: (B.F.S.) bert.sels@biw.kuleuven.be, (M.D.) michiel.dusselier@biw.kuleuven.be.

Notes

The authors declare no competing financial interest.

ACKNOWLEDGMENTS

M.D. acknowledges "FWO Vlaanderen" (Grant 1.1.955.10N) for financial support. The Research Council of the K.U. Leuven (IDO-3E090504) is also acknowledged. We are grateful to Karel Duerinckx for help with the in situ NMR. B.F.S. and F.D.P. acknowledge the Belgian Program on Interuniversity Attraction Poles initiated by the Belgian State, Prime Minister's office (Program P7/05) for financial support.

ABBREVIATIONS

MVG, EVG, and IVG: methyl, ethyl, and isopropyl vinyl glycolate, respectively; MMHB or EEHB: (m)ethyl-4-(m)-ethoxy-2-hydroxybutanoate; IIHB: isopropyl-4-isopropoxy-2-hydroxybutanoate; GA: glycolaldehyde; GADMA: glycolaldehyde dimethyl acetal; GAHA: glycolaldehyde hemiacetal; VG: vinyl glycolic acid; EtOH: ethanol; 2,4-DHB: 2,4-dihydroxybutanoic acid; HBL: α-hydroxy-γ-butyrolactone; IPA: isopropyl alcohol; MeOH: methanol; DMSO: dimethyl sulfoxide; PLLA: poly(L-lactic acid); PLLA-co-VG(x%): poly(L-lactic acid)-co-(vinyl glycolic acid) with x% of VG units in the copolymer; TG: thioglycerol; BM: benzyl mercaptan

REFERENCES

(1) Dusselier, M.; Van Wouwe, P.; Dewaele, A.; Makshina, E.; Sels, B. F. *Energy Environ. Sci.* **2013**, *6*, 1415.
(2) Carlos Serrano-Ruiz, J.; Dumesic, J. A. *Green Chem.* **2009**, *11*, 1101.
(3) Chheda, J. N.; Huber, G. W.; Dumesic, J. A. *Angew. Chem., Int. Ed.* **2007**, *46*, 7164.
(4) Corma, A.; Iborra, S.; Velty, A. *Chem. Rev.* **2007**, *107*, 2411.
(5) de Clippel, F.; Dusselier, M.; Van Rompaey, R.; Vanelderen, P.; Dijkmans, J.; Makshina, E.; Giebeler, L.; Oswald, S.; Baron, G. V.; Denayer, J. F. M.; Pescarmona, P. P.; Jacobs, P. A.; Sels, B. F. *J. Am. Chem. Soc.* **2012**, *134*, 10089.
(6) Aparicio, S.; Alcalde, R. *Green Chem.* **2009**, *11*, 65.
(7) Pereira, C. S. M.; Silva, V. M. T. M.; Rodrigues, A. E. *Green Chem.* **2011**, *13*, 2658.

(8) Auras, R., Lim, L.-T., Selke, S. E. M., Tsuji, H., Eds. *Poly(Lactic Acid): Synthesis, Structures, Properties, Processing, And Applications*; John Wiley & Sons, Inc.: New York, 2010.
(9) Shen, L.; Worrell, E.; Patel, M. *Biofuels, Bioprod. Bioref.* **2010**, *4*, 25.
(10) Gruber, P.; Henton, D. E.; Starr, J. In *Biorefineries-Industrial Processes and Products*; Wiley-VCH Verlag GmbH: Weinheim, 2008, p 381.
(11) Mecking, S. *Angew. Chem., Int. Ed.* **2004**, *43*, 1078.
(12) Drumright, R. E.; Gruber, P. R.; Henton, D. E. *Adv. Mater.* **2000**, *12*, 1841.
(13) Vink, E. T. H.; Rábago, K. R.; Glassner, D. A.; Gruber, P. R. *Polym. Degrad. Stab.* **2003**, *80*, 403.
(14) Gross, R. A.; Kalra, B. *Science* **2002**, *297*, 803.
(15) Tuck, C. O.; Pérez, E.; Horváth, I. T.; Sheldon, R. A.; Poliakoff, M. *Science* **2012**, *337*, 695.
(16) Moore, C. J. *Environ. Res.* **2008**, *108*, 131.
(17) Law, K. L.; Morét-Ferguson, S.; Maximenko, N. A.; Proskurowski, G.; Peacock, E. E.; Hafner, J.; Reddy, C. M. *Science* **2010**, *329*, 1185.
(18) Thompson, R. C.; Olsen, Y.; Mitchell, R. P.; Davis, A.; Rowland, S. J.; John, A. W. G.; McGonigle, D.; Russell, A. E. *Science* **2004**, *304*, 838.
(19) Rasal, R. M.; Janorkar, A. V.; Hirt, D. E. *Prog. Polym. Sci.* **2010**, *35*, 338.
(20) Holm, M. S.; Saravanamurugan, S.; Taarning, E. *Science* **2010**, *328*, 602.
(21) Holm, M. S.; Pagan-Torres, Y. J.; Saravanamurugan, S.; Riisager, A.; Dumesic, J. A.; Taarning, E. *Green Chem.* **2012**, *14*, 702.
(22) Dusselier, M.; Van Wouwe, P.; de Clippel, F.; Dijkmans, J.; Gammon, D. W.; Sels, B. F. *ChemCatChem.* **2013**, *5*, 569.
(23) Summerbell, R. K.; Rochen, L. K. *J. Am. Chem. Soc.* **1941**, *63*, 3241.
(24) Sasaki, M.; Goto, K.; Tajima, K.; Adschiri, T.; Arai, K. *Green Chem.* **2002**, *4*, 285.
(25) Richards, G. N. *J. Anal. Appl. Pyrol.* **1987**, *10*, 251.
(26) Vinu, R.; Broadbelt, L. J. *Energy Environ. Sci.* **2012**, *5*, 9808.
(27) Lin, Y.-C.; Huber, G. W. *Energy Environ. Sci.* **2009**, *2*, 68.
(28) Van de Vyver, S.; Geboers, J.; Jacobs, P. A.; Sels, B. F. *ChemCatChem* **2011**, *3*, 82.
(29) Geboers, J. A.; Van de Vyver, S.; Ooms, R.; Op de Beeck, B.; Jacobs, P. A.; Sels, B. F. *Catal. Sci. Technol.* **2011**, *1*, 714.
(30) Rinaldi, R.; Schuth, F. *Energy Environ. Sci.* **2009**, *2*, 610.
(31) Op de Beeck, B.; Geboers, J.; Van de Vyver, S.; Van Lishout, J.; Snelders, J.; Huijgen, W. J. J.; Courtin, C. M.; Jacobs, P. A.; Sels, B. F. *ChemSusChem* **2013**, *6*, 199.
(32) Van de Vyver, S.; Geboers, J.; Schutyser, W.; Dusselier, M.; Eloy, P.; Dornez, E.; Seo, J. W.; Courtin, C. M.; Gaigneaux, E. M.; Jacobs, P. A.; Sels, B. F. *ChemSusChem* **2012**, *5*, 1549.
(33) Rinaldi, R.; Schüth, F. *ChemSusChem* **2009**, *2*, 1096.
(34) Geboers, J.; Van de Vyver, S.; Carpentier, K.; Jacobs, P.; Sels, B. *Chem. Commun.* **2011**, *47*, 5590.
(35) Vitasari, C. R.; Meindersma, G. W.; de Haan, A. B. *Green Chem.* **2012**, *14*, 321.
(36) Wang, T.; Bowie, J. H. *Org. Biomol. Chem.* **2010**, *8*, 4757.
(37) Benner, S. A.; Kim, H.-J.; Kim, M.-J.; Ricardo, A. *Cold Spring Harbor Perspectives in Biology*; Cold Spring Harbor Laboratory Press: Cold Spring Harbor, NY, 2010.
(38) Weber, A. L.; Pizzarello, S. *Proc. Natl. Acad. Sci. U.S.A.* **2006**, *103*, 12713.
(39) Kim, H.-J.; Ricardo, A.; Illangkoon, H. I.; Kim, M. J.; Carrigan, M. A.; Frye, F.; Benner, S. A. *J. Am. Chem. Soc.* **2011**, *133*, 9457.
(40) Kofoed, J.; Reymond, J.-L.; Darbre, T. *Org. Biomol. Chem.* **2005**, *3*, 1850.
(41) Breslow, R. *Tetrahedron Lett.* **1959**, *1*, 22.
(42) Socha, R. F.; Weiss, A. H.; Sakharov, M. M. *J. Catal.* **1981**, *67*, 207.
(43) Weiss, A. H.; LaPierre, R. B.; Shapira, J. *J. Catal.* **1970**, *16*, 332.
(44) Ricardo, A.; Carrigan, M. A.; Olcott, A. N.; Benner, S. A. *Science* **2004**, *303*, 196.
(45) Lambert, J. B.; Gurusamy-Thangavelu, S. A.; Ma, K. *Science* **2010**, *327*, 984.
(46) Holm, T. *J. Chromatogr., A* **1999**, *842*, 221.
(47) Kim, K. W.; Woo, S. I. *Macromol. Chem. Phys.* **2002**, *203*, 2245.
(48) Collins, G. C. S.; George, W. O. *J. Chem. Soc. B* **1971**, *0*, 1352.
(49) Yaylayan, V. A.; Harty-Majors, S.; Ismail, A. A. *Carbohydr. Res.* **1998**, *309*, 31.
(50) Kofoed, J.; Machuqueiro, M.; Reymond, J.-L.; Darbre, T. *Chem. Commun.* **2004**, *0*, 1540.
(51) Burroughs, L.; Vale, M. E.; Gilks, J. A. R.; Forintos, H.; Hayes, C. J.; Clarke, P. A. *Chem. Commun.* **2010**, *46*, 4776.
(52) De, S. K.; Gibbs, R. A. *Tetrahedron Lett.* **2004**, *45*, 8141.
(53) Teesdale-Spittle, P. *Appl. Organomet. Chem.* **1993**, *7*, 293.
(54) Shigemasa, Y.; Taji, T.; Sakazawa, C.; Nakashima, R.; Matsuura, T. *J. Catal.* **1979**, *58*, 296.
(55) Kofoed, J.; Darbre, T.; Reymond, J.-L. *Chem. Commun.* **2006**, *0*, 1482.
(56) Centi, G., van Santen, R. A., Eds.; *Catalysis for Renewables: From Feedstock to Energy Production*; Wiley-VCH Verlag GmbH & Co. KGaA: Weinheim, 2007.
(57) Blunden, S. J.; Cusack, P. A.; Smith, P. J. *J. Organomet. Chem.* **1987**, *325*, 141.
(58) Roman-Leshkov, Y.; Davis, M. E. *ACS Catal.* **2011**, *1*, 1566.
(59) Hayashi, Y.; Sasaki, Y. *Chem. Commun.* **2005**, 2716.
(60) Moliner, M.; Roman-Leshkov, Y.; Davis, M. E. *Proc. Natl. Acad. Sci. U.S.A.* **2010**, *107*, 6164.
(61) Bermejo-Deval, R.; Assary, R. S.; Nikolla, E.; Moliner, M.; Román-Leshkov, Y.; Hwang, S.-J.; Palsdottir, A.; Silverman, D.; Lobo, R. F.; Curtiss, L. A.; Davis, M. E. *Proc. Natl. Acad. Sci. U.S.A.* **2012**, *109*, 9727.
(62) Roman-Leshkov, Y.; Moliner, M.; Labinger, J. A.; Davis, M. E. *Angew. Chem., Int. Ed.* **2010**, *49*, 8954.
(63) Gunther, W. R.; Wang, Y.; Ji, Y.; Michaelis, V. K.; Hunt, S. T.; Griffin, R. G.; Román-Leshkov, Y. *Nat. Commun.* **2012**, *3*, 1109.
(64) Miller, K. J.; Kitagawa, T. T.; Abu-Omar, M. M. *Organometallics* **2001**, *20*, 4403.
(65) Hall, R. H.; Stern, E. S. *J. Chem. Soc.* **1954**, 3388.
(66) Pescarmona, P. P.; Janssen, K. P. F.; Delaet, C.; Stroobants, C.; Houthoofd, K.; Philippaerts, A.; De Jonghe, C.; Paul, J. S.; Jacobs, P. A.; Sels, B. F. *Green Chem.* **2010**, *12*, 1083.
(67) Li, L.; Stroobants, C.; Lin, K.; Jacobs, P. A.; Sels, B. F.; Pescarmona, P. P. *Green Chem.* **2011**, *13*, 1175.
(68) Choudhary, V.; Mushrif, S. H.; Ho, C.; Anderko, A.; Nikolakis, V.; Marinkovic, N. S.; Frenkel, A. I.; Sandler, S. I.; Vlachos, D. G. *J. Am. Chem. Soc.* **2013**, *135*, 3997.
(69) Nikolla, E.; Román-Leshkov, Y.; Moliner, M.; Davis, M. E. *ACS Catal.* **2011**, *1*, 408.
(70) Bubb, W. A. *Concepts Magn. Reson., Part A* **2003**, *19A*, 1.
(71) Hammond, C.; Conrad, S.; Hermans, I. *Angew. Chem., Int. Ed.* **2012**, *51*, 11736.
(72) Bermejo-Deval, R.; Gounder, R.; Davis, M. E. *ACS Catal.* **2012**, *2*, 2705.
(73) Luo, H. Y.; Bui, L.; Gunther, W. R.; Min, E.; Román-Leshkov, Y. *ACS Catal.* **2012**, *2*, 2695.
(74) Corma, A.; Domine, M. E.; Nemeth, L.; Valencia, S. *J. Am. Chem. Soc.* **2002**, *124*, 3194.
(75) de Clippel, F.; Dusselier, M.; Van de Vyver, S.; Peng, L.; Jacobs, P. A.; Sels, B. F. *Green Chem.* **2013**, *15*, 1398.
(76) Sodergard, A.; Stolt, M. *Prog. Polym. Sci.* **2002**, *27*, 1123.
(77) Wang, M.; Radano, C. P.; Mackay, M. E.; McCabe, L. R.; Baker, G. L.; Smith, M. R., III *Polym. Prepr. (Am. Chem. Soc., Div. Polym. Chem.)* **2003**, *44*, 716.
(78) Jing, F.; Smith, M. R., III; Baker, G. L. *Macromolecules* **2007**, *40*, 9304.
(79) Liu, T.; Simmons, T. L.; Bohnsack, D. A.; MacKay, M. E.; Smith, M. R., III; Baker, G. L. *Macromolecules* **2007**, *40*, 6040.
(80) Yin, M.; Baker, G. L. *Macromolecules* **1999**, *32*, 7711.

(81) Espeel, P.; Goethals, F.; Du Prez, F. E. *J. Am. Chem. Soc.* **2011**, *133*, 1678.
(82) Koo, S. P. S.; Stamenović, M. M.; Prasath, R. A.; Inglis, A. J.; Du Prez, F. E.; Barner-Kowollik, C.; Van Camp, W.; Junkers, T. *J. Polym. Sci., Part A: Polym. Chem.* **2010**, *48*, 1699.
(83) Petton, L.; Ciolino, A. E.; Stamenović, M. M.; Espeel, P.; Du Prez, F. E. *Macromol. Rapid Commun.* **2012**, *33*, 1310.
(84) Ishaug-Riley, S. L.; Okun, L. E.; Prado, G.; Applegate, M. A.; Ratcliffe, A. *Biomaterials* **1999**, *20*, 2245.
(85) Paragkumar, N, T.; Edith, D.; Six, J.-L. *Appl. Surf. Sci.* **2006**, *253*, 2758.